Nonlinear Nano-Optics: Probing One Exciton at a Time

N. H. Bonadeo,[1,2] Gang Chen,[1] D. Gammon,[3] D. S. Katzer,[3] D. Park,[3] and D. G. Steel[2]

[1]*The Harrison M. Randall Laboratory of Physics, The University of Michigan, Ann Arbor, Michigan 48109*
[2]*The Center of Ultrafast Optical Science, The University of Michigan, Ann Arbor, Michigan 48109*
[3]*Naval Research Laboratory, Washington, D.C. 20375*

Coherent nonlinear optical spectroscopy of individual excitons in GaAs quantum dots is demonstrated and shows strong similarities with atoms in their coherent optical interaction, unlike higher dimensional heterostructures. The nonlinear response is dominated by an incoherent contribution (saturation) and a coherent contribution (population pulsations) of the single dot and compares well with present theory. The data shows that energy relaxation and dephasing rates are comparable, reflecting the absence of significant pure dephasing, and also demonstrate the presence of interdot energy transfer. [S0031-9007(98)07287-1]

PACS numbers: 71.35.−y, 73.20.Fz, 78.47.+p, 78.66.Fd

Recent studies of electron-hole excitation in quantum dots (QD) show the consequences of three-dimensional confinement including atomiclike δ-function density of states and increased exciton binding energy and oscillator strength. Using photoluminescence (PL) and various microprobing methods to eliminate spectral blurring, numerous groups have now reported sharp line spectra and excited states of individual QD's similar to atoms [1–4]. In this paper, we combine the breakthrough of single QD probing with the power of nonlinear optical spectroscopy in semiconductors [5] to observe the coherent nonlinear optical response of a single exciton confined in a QD potential. The measurements show the coherent nonlinear interaction with light is atomiclike in nature revealing that the dominant nonlinearity is state filling as predicted in earlier theoretical studies [6]. The work opens up a new direction of research for direct measurements of exciton dynamics in QD's (e.g., dephasing, energy relaxation, interdot coupling, etc.) and optical nonlinearities as well as taking the first step in the direction of demonstrating coherent control and fast switching for novel applications [7]. The data provide a measure of the energy relaxation rates and the dephasing rate and show the absence of significant pure dephasing processes at low temperature. The data also show the contribution to energy relaxation in some dots due to interdot energy transfer. Probing a single exciton demonstrates coherent optical coupling leading to population pulsations of single dots at frequencies above 15 GHz. The measurements show the profound effects of the complete discretization of the energy spectra to the resonant nonlinear response [6] demonstrating the similarity of these dots with atomic systems beyond linear response.

Measurements are made at $T = 6$ K on a narrow (42 Å) single molecular-beam epitaxy (MBE) grown GaAs quantum well with 250 Å $Al_{0.3}Ga_{0.7}As$ barriers. Growth interrupts at the interfaces lead to the formation of large monolayer-high islands [8] which localize excitons in QD

potentials that are 15 monolayers thick with lateral dimensions on the order of 40 nm [3]. Excitons in isolated QD's are probed by exciting through a 0.2–2.5 μm aperture in a 100-nm-thick Al mask deposited directly on the sample surface [3]. The sample is attached to a sapphire disk (*c*-axis normal) and the substrate removed with a liquid etch. Earlier PL and PLE studies of these structures have shown well-defined optical resonances of single quantum confined excitons characterized by an atomiclike spectrum of excited states determined by the details of the confinement potential [3].

The experimental approach to high resolution frequency domain coherent nonlinear laser spectroscopy in semiconductors has been discussed in numerous measurements (see, for example, [9]). Similar measurements in this system are challenging because of the low signal level from a single exciton and the relatively large background noise due to scattering from the metalized aperture. There is also a nonresonant background contribution to the nonlinear response, possibly arising from excitation outside the quantum well region (e.g., such as in the GaAs support layer.) Hence, a more sophisticated experimental approach was developed for these measurements and is discussed in detail elsewhere [10]. Briefly, the measurements are based on the use of two independently tunable optical fields, $E_1(\omega_1)$ and $E_2(\omega_2)$, supplied by two cw single frequency dye lasers which simultaneously excite the aperture. The lasers are frequency locked to separate temperature stabilized Fabre-Perot reference cavities and have a bandwidth of less than 1 MHz (4 neV) and a mutual bandwidth of 3 MHz. The fields are linearly polarized and parallel to a 110 axis to avoid complications due to fine structure splitting [3,11]. The relatively slow nonresonant background nonlinear response is suppressed by the use of high frequency amplitude modulation of the optical fields at 100 MHz and $100 + \delta$ MHz, respectively. The signal field, generated by the third order induced optical polarization, $P_{NL}^{(3)} = \zeta\chi^{(3)}E_1E_1^*E_2$ where $\chi^{(3)}$ is the nonlinear

1. REPORT DATE **20 OCT 1997**	2. REPORT TYPE	3. DATES COVERED **00-00-1997 to 00-00-1997**	
4. TITLE AND SUBTITLE **Nonlinear Nano-Optics: Probing One Exciton at a Time**		5a. CONTRACT NUMBER	
		5b. GRANT NUMBER	
		5c. PROGRAM ELEMENT NUMBER	
6. AUTHOR(S)		5d. PROJECT NUMBER	
		5e. TASK NUMBER	
		5f. WORK UNIT NUMBER	
7. PERFORMING ORGANIZATION NAME(S) AND ADDRESS(ES) **Naval Research Laboratory,Washington,DC,20375**		8. PERFORMING ORGANIZATION REPORT NUMBER	
9. SPONSORING/MONITORING AGENCY NAME(S) AND ADDRESS(ES)		10. SPONSOR/MONITOR'S ACRONYM(S)	
		11. SPONSOR/MONITOR'S REPORT NUMBER(S)	
12. DISTRIBUTION/AVAILABILITY STATEMENT **Approved for public release; distribution unlimited**			
13. SUPPLEMENTARY NOTES			
14. ABSTRACT			
15. SUBJECT TERMS			

16. SECURITY CLASSIFICATION OF:			17. LIMITATION OF ABSTRACT **Same as Report (SAR)**	18. NUMBER OF PAGES **4**	19a. NAME OF RESPONSIBLE PERSON
a. REPORT **unclassified**	b. ABSTRACT **unclassified**	c. THIS PAGE **unclassified**			

susceptibility and ζ is a constant, is then homodyne detected with the transmitted $E_2(\omega_2)$ field and provides a nearly background free signal. Physically, this measurement is similar to traditional differential transmission measurements when $\omega_1 \sim \omega_0$ (where E_1 is the pump and E_2 is the probe) except, as discussed below, for the important limit $|\omega_1 - \omega_2| \lesssim \Gamma_{\mathrm{rel}}$, where Γ_{rel} is the energy relaxation rate; here, the effects of coherent coupling in the spectral response become important showing atomiclike behavior with new physical information.

The fully degenerate (i.e., $\omega_1 = \omega_2$) nonlinear response as a function of frequency, which reports on the spectrum of the nonlinear excitation, is shown in the top curve in Fig. 1(b). For comparison, Fig. 1(a) shows the PL spectrum excited at 1.633 eV. In many cases, resonances seen in the PL (as extensively discussed in [1–3]) are also seen in the nonlinear spectrum. However, we note that, as in the comparison between PL and PLE spectra [3], there

are differences between the spectra which reflect important details of the electronic excitation. Indeed, the relative magnitude of the nonlinear spectral response depends not only on the dipole coupling and linewidth as in the linear response (absorption), it also depends on the inverse of the energy relaxation rate, as the analysis below shows. Resonances in the degenerate NL spectra can be well fit to a Lorentzian squared [Fig. 1(b); left inset] as expected from the analysis for isolated homogeneously broadened excitons.

For a simple resonant system, the signal strength of the nonlinear response goes linearly with intensity I_1 because the homodyne-detected lowest order contribution to the nonlinear response corresponds to the third order susceptibility [right inset of Fig. 1(b)]. At higher powers the response saturates and leads to power dependent spectral linewidths. All spectral data were obtained in the low power linear region. From the slope of the linear region, the imaginary part of the third order susceptibility is determined to be $\mathrm{Im}\,\chi^{(3)} \sim 0.03$ esu, assuming a localization length of order 40 nm [3].

One of the particularly powerful features of coherent nonlinear spectroscopy is that it probes the existence and nature of interactions; for example, in higher dimensional systems, this spectroscopy method shows the presence of strong exciton-exciton interactions due to Coulomb coupling (see, for example, [12]). In QD systems, we see that the strong confinement leads to profoundly different behavior. The three lower spectra shown in Fig. 1(b) are obtained by fixing the frequency of $E_1(\omega_1)$ at the resonances ω_A, ω_B, and ω_C located by the open arrows corresponding to resonances in the degenerate nonlinear response and scanning the frequency of $E_2(\omega_2)$. The experiments, which report on the response at ω_2 induced by the excitation at ω_1, show that in general only the directly excited dots have a strong response indicating the lack of interactions between excitons formed in different QD's. Tuning ω_1 off the QD resonance reduces the signal to the background level. It also shows (described in detail in Fig. 2) that the dominant nonlinearity is state filling, which results in a saturation of the effective oscillator strength. We do not observe contributions from line broadening or frequency shift characteristic of other many-body effects seen in higher dimensional systems [12]. The data, in addition, are profoundly different from studies in wide quantum wells where exciton localization is weak and phonon assisted migration leads to spectral diffusion and excitation of a broad energy distribution of localized excitons at lower energy [13]. We note that measurements with orthogonal polarizations (discussed in detail elsewhere [10]), while leading to complications due to fine structure splitting [3,11], do not show the changes in intensity or dephasing rate seen in quantum wells [14].

Further information regarding the interaction with coherent radiation and the nature of the electronic excitation is obtained by measuring with high resolution the line shape of the response as a function of ω_2 for
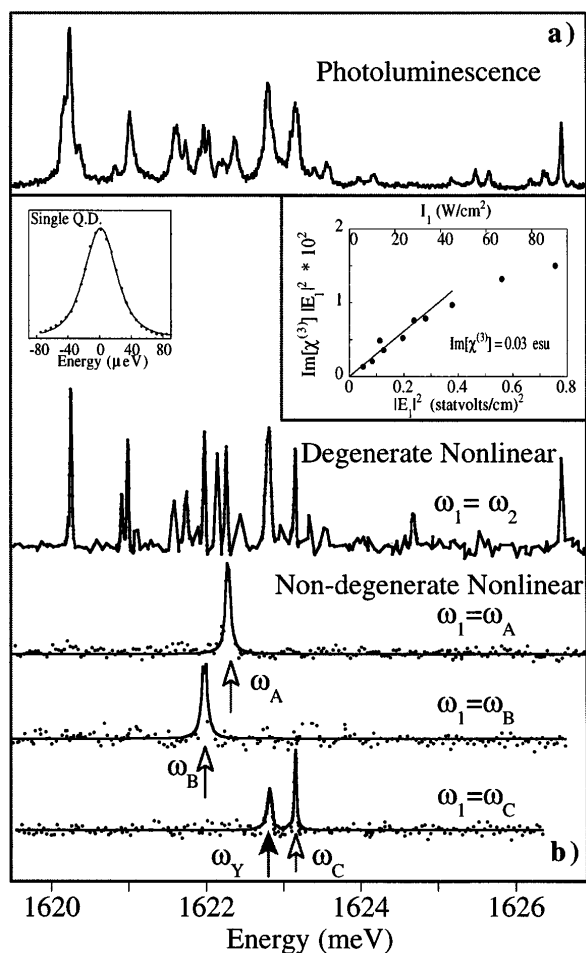

FIG. 1.   (a) The PL spectrum through a 0.5 μm aperture at low resolution ($\sim$50 μeV). (b) Top curve: the fully degenerate nonlinear spectrum (i.e., $\omega_1 = \omega_2$). Bottom curves: The nonlinear response as a function of ω_2 when ω_1 remains fixed at the position indicated by the arrow. (See test for discussion of resonance at ω_γ). (Right inset) The power dependence of the signal. (Left inset) A Lorentzian squared fit to a high resolution degenerate nonlinear response.

$|\omega_2 - \omega_2| \lesssim \Gamma_{rel}$ and $\omega_1 \sim \omega_0$ where $\hbar\omega_0$ corresponds to the transition energy of a specific resonance. Under these conditions, the effects of coherent optical coupling become important and lead to new physical measurements. Figure 2 shows the spectra obtained as a function of ω_2 for detunings of ω_1 relative to the peak of the resonance (ω_0). Interestingly, the data show that the peak tracks ω_1 but occurs between the peak of the degenerate

nonlinear response and ω_1. In addition, a strong asymmetry develops as the detuning from resonance increases.

To provide physical insight we examine the nonlinear polarization to third order in the optical fields. As previously reported [6], the expression is very similar to that for a two-level system in the limit of fully resonant excitation in which nonresonant contributions can be ignored (e.g., the biexciton [1,15]):

$$\tilde{P}_{NL}^{(3)} = \frac{-2|\mu|^4 i \tilde{E}_1 \tilde{E}_1^* \tilde{E}_2}{(8\hbar^3)(\gamma + i\Delta_2)} \left[\left(\frac{\Gamma_{rec}^{-1}}{\gamma + i\Delta_1} + c.c. \right) + \frac{1}{\Gamma_{rel} + i(\Delta_2 - \Delta_1)} \left(\frac{1}{\gamma - i\Delta_1} + \frac{1}{\gamma + i\Delta_2} \right) \right], \quad (1)$$

where $(\tilde{E}_i)$ represents the amplitude of the field i, μ is the dipole moment, and Δ_i is the detuning of the field i from the resonance ω_0. Γ_{rel} corresponds to the recombination rate due to spontaneous emission and other decay processes such as energy transfer, etc.; $T_2^{-1} \equiv \gamma = \Gamma_{rel}/2 + \gamma_{ph}$ is the dephasing rate of the optically induced coherence (in analogy with the inverse of the T_2 time scale in spin systems [16]). γ_{ph} is the so-called pure dephasing due to processes that affect only the relative phases of the eigenstates of the transition (elastic phonon scattering, etc.) without resulting in energy relaxation. The homodyne detected response reports on the imaginary contribution to Eq. (1).

The first term in the above expression is the usual term in standard pump-and-probe experiments where the field, $E_1(\omega_1)$, excites the system leading to a change in the absorption and dispersion reflecting the saturation of the resonance. The change, proportional to $E_1(\omega_1)E_1^*(\omega_1)$, is sensed by the field $E_2(\omega_2)$. As can be seen from

the denominators of Eq. (1), the peak of the response as a function of ω_2 occurs at ω_0 and does not track with the pump frequency. The second term corresponds to a coherent interaction in the sample and arises from the optical response induced by the coherent coupling between the two fields. This contribution, proportional to $E_1^*(\omega_1)E_2(\omega_2)$, leads to a temporal modulation of the excitation (population pulsations [16]), at the difference frequency $\omega_2 - \omega_1$.

Figure 3 shows the calculated spectrum for the degenerate and nearly degenerate response for two limiting cases. In both cases, the degenerate response is given by the square of a Lorentzian whose width is given by γ. In the absence of pure dephasing ($\gamma_{ph} = 0$), Fig. 3(a) shows the nearly degenerate response is Lorentzian squared when $\omega_1 = \omega_0$, but develops into an interference line shape with the peak of the response following but lagging ω_1. A similar result is obtained when γ_{ph} is comparable to the energy
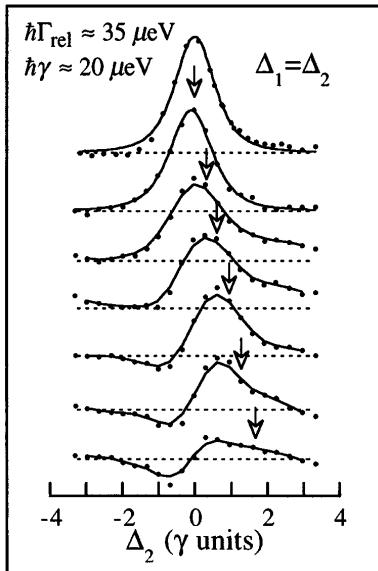

FIG. 2. High resolution spectrum of the degenerate (upper curve) and nearly degenerate nonlinear response of a single QD resonance as a function of $\Delta_2 = \omega_2 - \omega_0$ for fixed detunings of $\Delta_1 = \omega_1 - \omega_0$ (located by the arrow). The data show a clear tracking of the peak of the response, though lagging, with the position of ω_1. (Solid lines are a guide to the eye.)
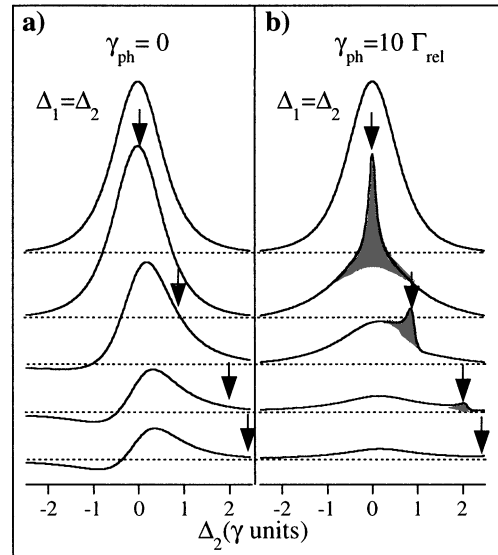

FIG. 3. The nonlinear response obtained from the imaginary part of Eq. (1) for both the degenerate case (top curves), and various nondegenerate cases. The response is plotted as a function of $\Delta_2 = \omega_2 - \omega_0$ for fixed detunings of $\Delta_1 = \omega_1 - \omega_0$ (located by the arrow) for two limiting cases: (a) $\gamma_{ph} = 0$ and (b) $\gamma_{ph} = 10 \Gamma_{rec}$. The shading in (b) differentiates between the two resonant contributions.

relaxation rate. However, when $\gamma_{\rm ph} \gg \Gamma_{\rm rel}/2$, we find that the nearly degenerate response develops a sharp resonance on top of a much broader resonance. The width of the narrow resonance is given by the energy relaxation rate, while the width of the broad resonance is given by γ. Moreover, the broad resonance is centered at $\omega_2 = \omega_0$ while the sharp resonance occurs at $\omega_2 = \omega_1$.

A comparison between Figs. 2 and 3 shows that the response is similar to the case of Fig. 3(a), hence we conclude that $\gamma_{\rm ph} \lesssim \Gamma_{\rm rec}$. Furthermore, the peak of the nearly degenerate response tracks ω_1 but occurs between ω_0 and ω_1. This is different from the spectral hole burning that is observed in inhomogeneously broadened systems [13]. The behavior in Fig. 2 confirms that the system is homogeneously broadened as expected for an isolated dot and that in the limit of resonant excitation it behaves as a two-level system as anticipated by the theory [6].

More interesting is the development of a strong interference effect in the ω_2-spectral profile as ω_1 is tuned away from ω_0. This is the first such report of this line shape in a semiconductor heterostructure and is a classic line shape seen in atomic systems that is the direct result of coherent coupling between the two optical fields when $|\omega_1 - \omega_2| \lesssim \Gamma_{\rm rel}$. This coupling leads to population pulsations at the difference frequency $|\omega_1 - \omega_2|$ which interfere with scattering from the ordinary incoherent differential transmission type behavior given by the first term in Eq. [1]. This interference effect is the onset of two-beam coupling which, in the limit of $I/I_{\rm sat} \geq 1$ and $|\omega_1 - \omega_0| \gg T_2^{-1}$ leads to energy transfer between the fields [16]. The population pulsations are in excess of 15 GHz.

A quantitative analysis of the line shapes based on Eq. (1) allows us to estimate both the dephasing time for the excitation *and* the energy relaxation time. A Lorentzian squared fit to the degenerate response in Fig. 2 gives a dephasing time of 32 ± 1 psec ($\hbar\gamma \approx 20~\mu eV$). Using this result, we fit the complete nonlinear response to obtain a first measurement of the energy relaxation time in a single QD: $\Gamma_{\rm rel}^{-1} = 19 \pm 3$ psec. While there is significant variation between dots, we can conclude that the role of extra dephasing mechanisms in these systems at low temperature is comparable at most to the dephasing created by energy relaxation in sharp contrast with what is found in bulk and wide quantum well semiconductors.

Finally, we describe results shown in the last curve of Fig. 1(b) in which the pump is tuned to one resonance and the scanner probe reveals a secondary resonance (at ω_γ). These secondary resonances, often observed, can be due to excited states of the same QD. However, in a few cases including the peak at ω_γ in Fig. 1(b), these secondary resonances arise from energy transfer to a different QD. Separate measurements with excitation field (ω_1) located at ω_γ show no response at ω_C, confirming that the coupling is due to energy transfer from the state at ω_C

to the state at ω_γ. Based on the measurements of the total energy relaxation time and the relative strengths of the response, a straightforward calculation of the transfer rate for this case gives an estimate of $\sim 1.4 \times 10^{10}~{\rm sec}^{-1}$. The capability to coherently pump and probe single excitonic states either in the same QD or in different QD's is unique and will be important for further studies to determine the mechanisms of various energy relaxation and transfer processes.

In summary, this work reports the coherent nonlinear optical response of a single QD. The results demonstrate major differences between the coherent nonlinear optical interactions in these systems compared to those observed in higher dimensional systems and extend the similarity to atomic systems beyond the atomiclike energy level spectrum. The measurements serve as the first step in more complex studies such as demonstrating coherent optical control of a single QD and related physical phenomena such as Rabi flopping.

[1] K. Brunner *et al.,* Phys. Rev. Lett. **73**, 1138 (1994).

[2] H. F. Hess *et al.,* Science **264**, 1740 (1994).

[3] D. Gammon *et al.,* Phys. Rev. Lett. **76**, 3005 (1996); Science **273**, 87 (1996); **277**, 85 (1997).

[4] D. Hessman *et al.,* Appl. Phys. Lett. **69**, 749 (1996).

[5] J. Shah, *Ultrafast Processes in Semiconductors and Semiconductor Nanostructures* (Springer, Berlin, 1996).

[6] S. Schmitt-Rink, D. A. B. Miller, and D. S. Chemla, Phys. Rev. B **35**, 8113 (1987); L. Banyai *et al.,* Phys. Rev. B **38**, 8142 (1988); Y. Z. Hu, M. Lindberg, and S. W. Koch, Phys. Rev. B **42**, 1713 (1990); T. Takagahara, Phys. Rev. B **36**, 9293 (1987).

[7] A. Ekert and R. Jozsa, Rev. Mod. Phys. **68**, 733 (1996).

[8] D. Gammon, B. V. Shanabrook, and D. S. Katzer, Phys. Rev. Lett. **67**, 1547 (1991).

[9] H. Wang *et al.,* Phys. Rev. Lett. **69**, 804 (1992).

[10] N. Bonadeo *et al.* (unpublished).

[11] S. V. Gupalov, E. L. Ivchenko, and V. Kavokin, JETP **86**, 388 (1998).

[12] H. Haug and S. W. Koch, *Quantum Theory of the Optical and Electronic Properties of Semiconductors* (World Scientific, Singapore, 1993); S. Schmitt-Rink, D. S. Chemla, D. A. B. Miller, Adv. Phys. **38**, 89–188 (1989); H. Wang *et al.,* Phys. Rev. Lett. **71**, 1261 (1993).

[13] H. Wang, M. Jiang, and D. G. Steel, Phys. Rev. Lett. **65**, 1255 (1990).

[14] R. Eccleston *et al.,* Solid State Commun. **86**, 93 (1993); W. Schäfer *et al.,* Phys. Rev. B **53**, 16 429 (1996).

[15] O. Heller, Ph. Lelong, and G. Bastard, Phys. Rev. B **56**, 4702 (1997).

[16] P. Meystre and M. Sargent, *Elements of Quantum Optics* (Springer-Verlag, Berlin, 1990).